Precambrian Research 389 (2023) 107032

Contents lists available at ScienceDirect

Precambrian Research

journal homepage: www.elsevier.com/locate/precamres

Ca. 830 Ma alkaline mafic dykes in the southeastern Guizhou Province, South China: New constraints on the Neoproterozoic evolution of the Yangtze Block

Hong-Peng Fan [a], Jia-Xi Zhou [a,b,*], Zhi-Long Huang [a,*], Tao Wu [c,d], Hao Zhang [b]

[a] State Key Laboratory of Ore Deposit Geochemistry, Institute of Geochemistry, Chinese Academy of Sciences, Guiyang 550081, China
[b] Key Laboratory of Critical Minerals Metallogeny in Universities of Yunnan Province, School of Earth Sciences, Yunnan University, Kunming 650500, China
[c] Ocean College, Zhejiang University, Zhoushan 316021, China
[d] Hainan Institute of Zhejiang University, Building 11, Yonyou Industrial Park, Yazhou Bay Science and Technology City, Yazhou District, Sanya, Hainan Province 572025, China

ARTICLE INFO

Keywords:
Neoproterozoic
Alkaline magmatism
Tectonic evolution
South China

ABSTRACT

The Neoproterozoic alkaline mafic rocks in the Yangtze Block are critical to investigate the magmatic and tectonic evolution of South China. However, these rocks are rarely exposed. We here present a detailed study of ca. 830 Ma alkaline mafic dykes newly identified from a drilled borehole at the Nage area in the southern Yangtze Block. The dykes have SIMS zircon U-Pb ages of 827 ± 8 Ma. They show coherent variations in major and trace elements, characterized by enrichment in LREE and incompatible elements and no significant Nb-Ta and Zr-Hf anomalies, suggesting that their parental magmas have experienced varying degrees of fractionation crystallization with negligible crustal contamination. Modeling calculations based on their $\varepsilon_{Nd}(T)$ values (-0.55–3.23), SiO_2 contents (48.38–53.61 wt%) and elemental ratios (e.g., La/Ta and Nb/La) suggest that the Nage mafic dykes were probably generated from an asthenospheric mantle with previously input of a plume-derived enrich component occurred within the source region rather than during ascent. Rocks from the Nage dykes exhibit OIB-like trace element and REE patterns as well as trace elemental compositions, which are different from arc-related igneous rocks but similar to alkaline basalts and mafic dykes formed in mantle plume related rifting systems around the world. In combination with tectonostratigraphic evidences, the Nage dykes in this study are suggested to have been generated in an intraplate rift which was probably induced by a mantle plume beneath the Yangtze Block.

1. Introduction

The Yangtze Block, one of the major Precambrian blocks in China, has experienced an unique and complex tectonic history closely associated with the supercontinent cycles since Paleoproterozoic time (e.g., Li et al., 1995, 2008a,2014; Zhao et al., 2002; Zhao and Cawood, 2012; Meert and Santosh, 2017; Yao et al., 2019; Fan et al., 2020; Zhao and Wang, 2021). Nevertheless, controversial interpretations (e.g. plume model, subduction model, or intraplate rifting-related model) for the recurrently orogenic and magmatic events, especially those in Neoproterozoic era, have made the evolution history of the Yangtze Block hotly debated, which consequently results in a large uncertainty of its position in the Neoproterozoic supercontinent Rodinia (e.g., Wang et al., 2007a, 2019; Zhang et al., 2013a; Li et al., 2014; Zhao et al., 2011, 2018).

Neoproterozoic igneous rocks are widespread in the Yangtze Block, and are characterized by voluminous granitoids and many mafic–ultramafic plutons with sparse intermediate rocks (Fig. 1a and Fig. 2.) (Zhou et al., 2002a, 2004; Li et al., 2003, 2014; Zheng et al., 2007; Zhang and Zheng, 2013; Zhao et al., 2018, 2021). They are considered variably to have been formed within plume (Li et al., 1999), subduction (Zhou et al., 2002a; Zhao et al., 2011), or intraplate rifting-related tectonic settings (Zheng et al., 2007). The plume model suggests that these igneous rocks were products of multi-stage plume-induced magmatisms (850–830 Ma, 830–795 Ma and 780–745 Ma) (Li et al., 1999, 2007,2008a; Wang and Li, 2003; Wang et al., 2007a; Yang et al., 2015; Wu et al., 2018a, b, 2022). In contrast, the subduction model suggests that the early to middle Neoproterozoic calc-alkaline igneous

* Corresponding authors.
E-mail addresses: zhoujiaxi@ynu.edu.cn (J.-X. Zhou), huangzhilong@vip.gyig.ac.cn (Z.-L. Huang).

https://doi.org/10.1016/j.precamres.2023.107032
Received 7 November 2022; Received in revised form 12 March 2023; Accepted 14 March 2023
Available online 28 March 2023

rocks resulted from the oceanic slab subduction until ca. 810 Ma (Zhou et al., 2002a; Wang et al., 2013a; Yao et al., 2014a, b; Lin et al., 2016; Zhao et al., 2018). The subduction model also proposed a back-arc extension that occurred after ca. 830 Ma (Wang et al., 2006, 2012b; Zhao et al., 2011). The intraplate rifting model suggests an arc-continent collision occurred during the early Neoproterozoic, followed by an 830–800 Ma post-collisional extension and a 780–740 Ma continental rifting (Wu et al., 2006; Zheng et al., 2007). Therefore, all these models emphasize an important tectonic event occurred at ca. 830 Ma, and thus these middle Neoproterozoic igneous rocks are crucial to our

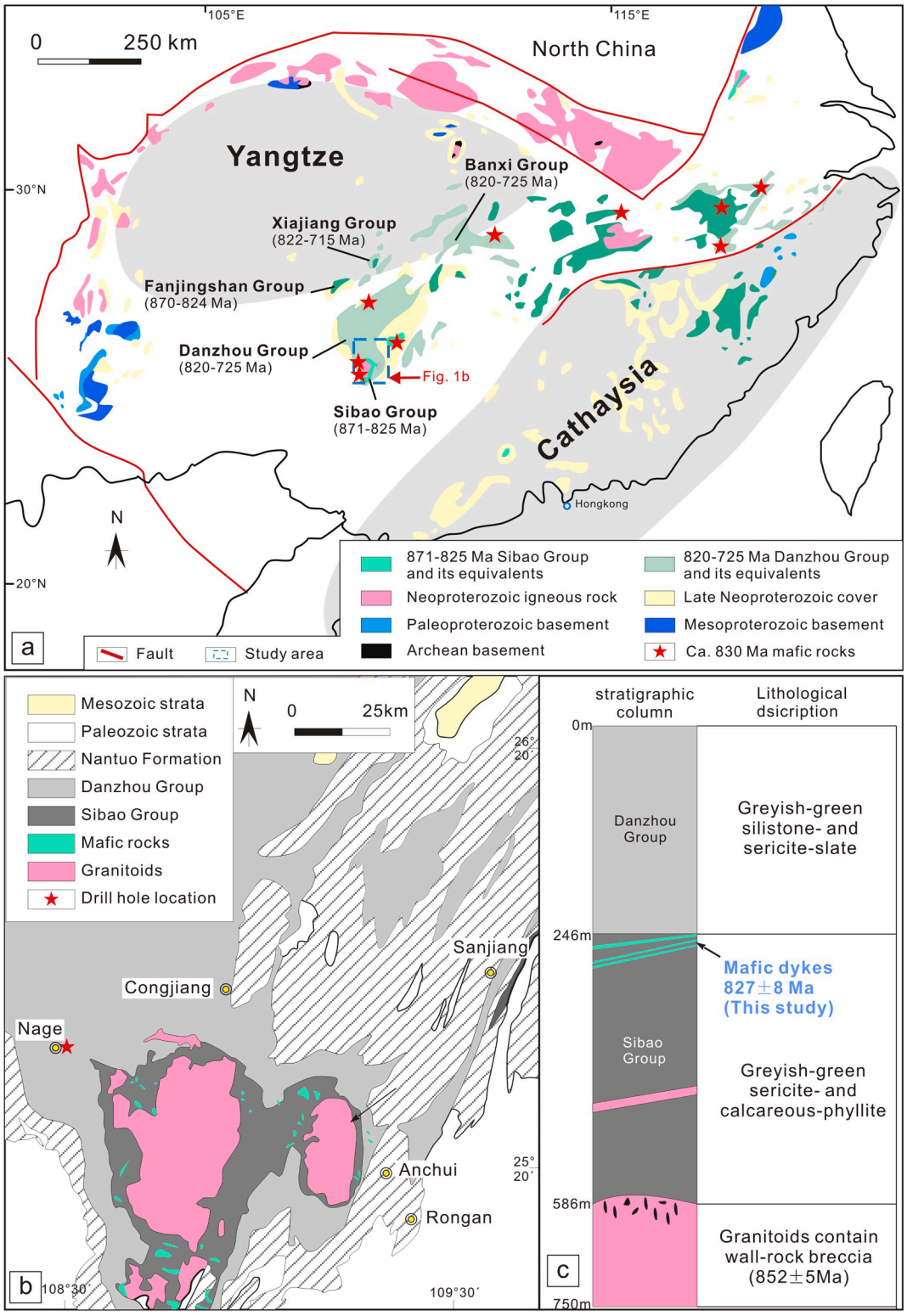

Fig. 1. A) simplified map of south china (revised from Li et al., 2010b, Yin et al., 2013; Wang et al., 2019); b) simplified geological map of the Nage area (after Wu et al., 2018b) and c) simplified stratigraphic column according to drill holes. Ca. 830 Ma mafic rocks in the Yangtze Block were reported by Ge et al. (2001), Wang et al. (2007a, 2019), Li et al. (2008a, 2016), Zhou et al. (2009), Zhang et al. (2012, 2013b), Zhao and Zhou (2013), Yao et al. (2014a), Zhao and Asimow (2014), and Wu et al. (2022).

understanding of tectonic evolution of South China.

Ca. 830 Ma calc-alkaline magmatic rocks in the Yangtze Block have long been studied (Fig. 1a and 2) (Li et al., 1999; Ge et al., 2001; Wu et al., 2006, 2022; Wang et al.,2007a, 2019; Li et al., 2008a, 2013,2016; Zhou et al., 2009; Zhao et al., 2011, 2018; Yin et al., 2013; Zhao and Zhou, 2013; Zhang et al., 2013b; Zhao and Asimow, 2014; Yao et al., 2014a; Chen et al., 2015, 2018; Sun et al., 2018; Wu et al., 2022). However, their tectonic setting has been debated regarding the arguments of subduction-related collisional vs post-collisional extension environments (Wang et al., 2007a, 2019; Li et al., 2008a, 2016; Zhao and Zhou, 2013; Zhang et al., 2012, 2013b; Zhao and Asimow, 2014; Yao et al., 2014a; Wu et al., 2022). Previous studies mostly emphasized on calc-alkaline felsic rocks which are widely exposed in the Yangtze Block. It is well known that alkaline mafic rocks is more sensitive to record deep magma source information and crustal-mantle interactions, and thus is critical to the investigation of magma petrogenesis and tectonic background (e.g., Li et al.,2015; Zhu et al., 2008). However, synchronous alkaline mafic rocks in the region are extremely sparse (Fig. 1a and Fig. 2.). In this contribution, we present a detailed study of ca. 830 Ma alkaline mafic dykes discovered by drillings at the Nage area in the southern Yangtze Block (Fig. 1b-c) to address their petrogenesis and tectonic background and to provide new clues to reveal Neoproterozoic evolution history of the Yangtze Block.

2. Geological background

The South China Craton consists of the Yangtze and the Cathaysia blocks (Fig. 1a). In the Yangtze Block, Archean to Mesoproterozoic basement rocks has been identified mainly on the northern and southwestern margins of the Block (Fig. 1a) (e.g., Li et al., 2014; Fan et al., 2020; Cui et al., 2021 and references therein). The oldest supracrustal rocks in the studied region are made up of an Early Tonian stratum and a Late Tonian sequence with a regional angular unconformity between them (Wang et al., 2007a, 2019; Zheng et al., 2008; Zhang et al., 2012, 2019; Li et al., 2014 and references therein). The regional angular unconformity is interpreted to reflect a rapid continental uplift attributed to a mantle plume (Li et al., 1999; Wang et al., 2007a; Li et al., 2014 and references therein) or a Neoproterozoic orogeny named the Jiannan orogeny that amalgamated the Yangtze and the Cathaysia blocks (Wang et al., 2007b; Zhao et al., 2011; Zhang et al., 2019 and references therein). The Early Tonian stratum, represented by the Sibao, Fanjingshan and Lengjiaxi groups, is composed of a unit of greenschist-facies metamorphosed siltstone, slate, sandstone and phyllite with small amounts of volcaniclastic, tufaceous and volcanic interlayers. Studies on detrital zircon and stratigraphic correlation indicated that the Sibao Group and its equivalents were probably deposited between 871 and 825 Ma (e.g., Wang et al., 2007b, 2012a,2014; Zhao et al., 2011; Li et al., 2014; Zhang et al., 2019 and references therein). The Late Tonian sequence, represented by the Danzhou, Xiajiang and Banxi groups, is mainly composed of metamorphosed sandstone and conglomerate, with small amounts of carbonate rock and igneous rocks, has been suggested to be deposited at ~820–715 Ma (e.g., Wang and Li, 2003; Wang et al., 2007a, 2019; Zheng et al., 2008; Li et al., 2014; Zhang et al., 2019 and references therein). Neoproterozoic magmatic rocks are widespread in the studied area (Fig. 1b). Among them, the exposed mafic–ultramafic rocks have ages ranging from 855 to 812 Ma (Li, 1999; Wang et al., 2006, 2012c; Zhou et al., 2017). Several alkaline mafic dykes were identified in this study from a borehole drilled for mineral exploration at the Nage area (Figs. 1 and 3a). They intruded siliceous rock and metasandstone of the Sibao Group (Fig. 1c and 3a). The dykes are fine- to medium-grained dolerites with width of 100–150 cm (Fig. 3a). Most samples from these dykes have suffered variable degrees of alteration (Fig. 3b-3c). However, they still show primary igneous texture and contain mainly plagioclase (mostly albitized) and clinopyroxene (Fig. 3b-3c).

3. Sampling and analytical methods

Eighteen dolerite samples were collected from a drilled borehole at the Nage area (Fig. 1b). The samples have been trimmed to remove their surfaces and expose the freshest parts which were then used for the preparation of thin sections and powders. These collected samples were all used for the following analysis.

Zircons were separated from a big sample made up of four samples (NG-19, NG-45, NG-46 and NG47) with each about 0.5–1 kg. Zircon grains were obtained with conventional heavy liquid plus magnetic methods and subsequent handpicking under binocular microscopes. The collected grains were then installed in an epoxy resin discs. Zircon grains

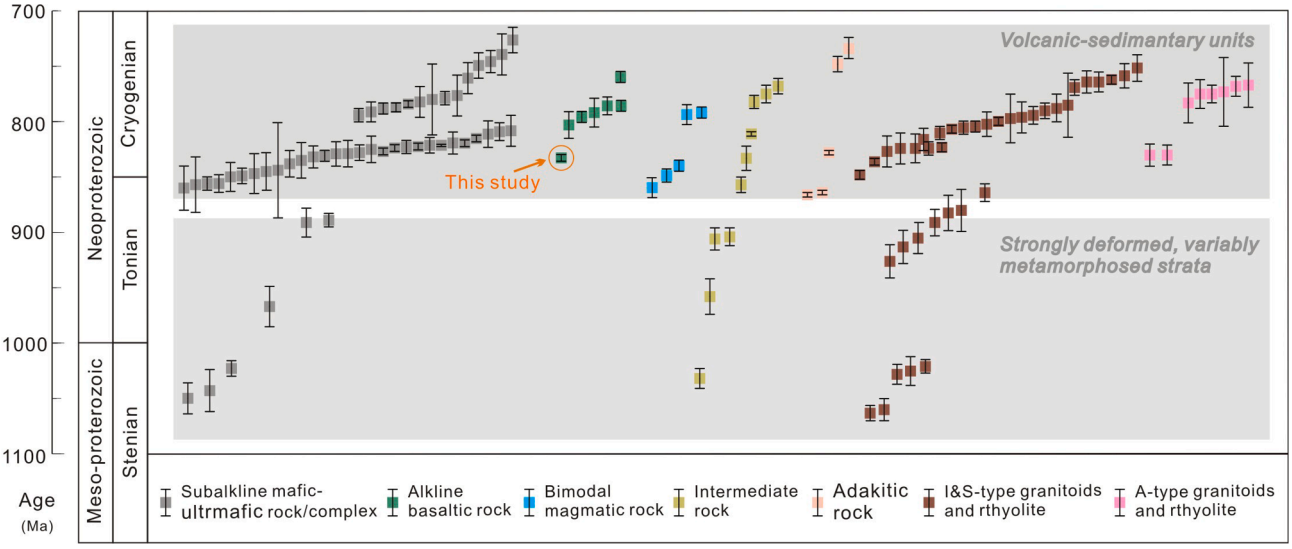

Fig. 2. Diagram of Zircon U-Pb and ^{40}Ar-^{39}Ar ages for magmatic rocks emplaced during 1100 Ma to 700 Ma in the Yangtze Block. Ages and errors are from Li et al. (1999, 2002, 2003, 2008a,b,c, 2009, 2010a,b,c, 2013, 2021); Ge et al. (2001); Zhou et al. (2002a,b, 2006, 2007, 2017, 2018); Mou et al. (2003); Zhu et al. (2006, 2007, 2008, 2016); Wang et al. (2006, 2007a, 2008, 2010, 2012b,c, 2016, 2019), Greentree et al. (2006); Wu et al. (2006); Zhao and Zhou (2007, 2008, 2009, 2013); Geng et al. (2007); Ye et al. (2007); Lin et al. (2007); Zhang et al. (2007, 2012, 2013b,c, 2017); Huang et al. (2008, 2009); Zhao et al. (2008); Chen et al. (2009, 2014, 2015, 2018)); Du et al. (2014); Ye et al. (2014b); Yang et al. (2017); Lyu et al. (2017); Sun et al. (2018); Lu et al. (2022).

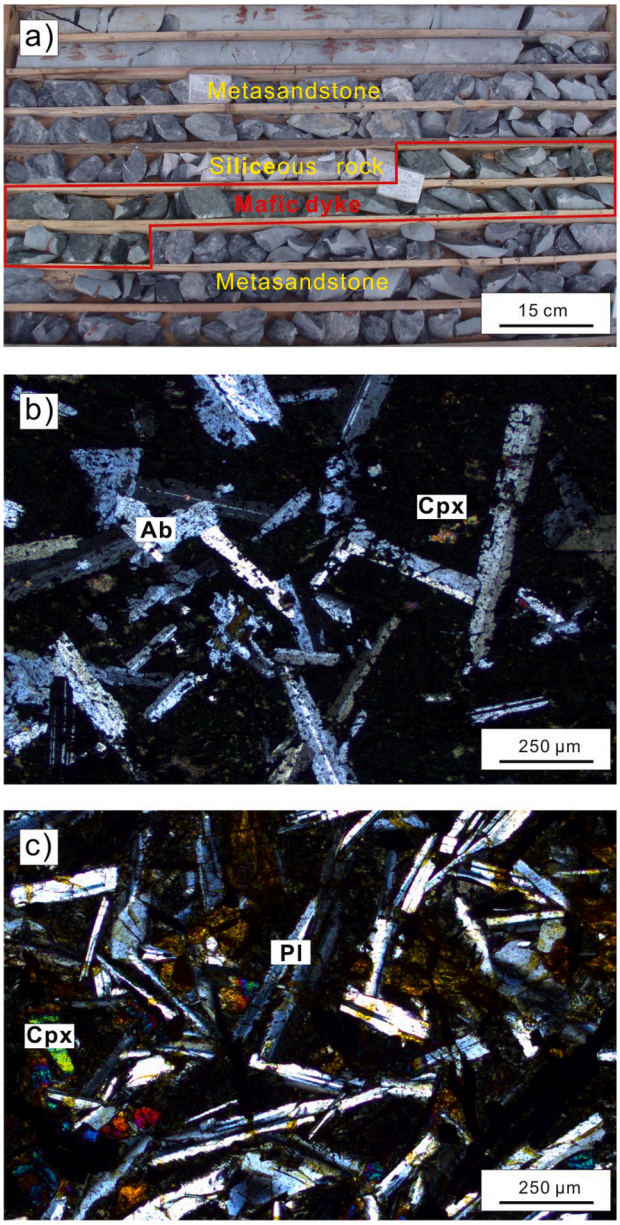

Fig. 3. A) photo of drill core samples showing that the nage mafic dyke intruded siliceous rock and metasandstone of the sibao group. microscopic photographs of representative samples collected from the nage mafic dykes. b) sample that have suffered significant alteration and c) relatively fresh sample. pl = plagioclase, Cpx = clinopyroxene, Ab = albite.

used for dating were selected based on their external and internal structures reveal by cathodoluminescence images and backscattered electron photos. Zircon U-Th-Pb isotopic compositions were analyzed on the Cameca IMS 1280 large-radius SIMS at the Institute of Geology and Geophysics, Chinese Academy of Sciences. Analytical and data processing procedure has been reported detailedly by Li et al. (2009). Detailed SIMS U-Pb dating results are given in Supplementary Table S1.

Whole-rock major oxide contents were analyzed on the X-ray fluorescence spectrometers at the State Key Lab of Ore Deposit Geochemistry (SKLODG), Institute of Geochemistry, Chinese Academy of Sciences. The relative standard derivation was less than 5 %. Whole-rock trace elements were determined using the PlasmaQuant MS Elite ICP-MS at SKLODG. Detailed analytical procedures can be found in Qi et al. (2000). The relative standard derivation was less than 10 %. Analysis results are shown in Supplementary Table S2.

During the Neodymium isotopic analysis, powder samples were dissolved with HF + HNO_3 acid in high-pressure Teflon bombs at the super–clean laboratory of SKLODG. Nd fractions were then separated by cation and HDEHP columns. Nd isotope was determined using a TIMS - Triton at SKLODG. The $^{143}Nd/^{144}Nd$ ratios of the BCR-2 standard were used for analytical quality control. Its $^{143}Nd/^{144}$ Nd values was measured at 0.512635 ± 0.000006 (2σ) during this study, which is within its recommended values (e.g., 0.512629 ± 0.000008 (2σ), Raczek et al., 2003). Detailed analysis results are list in Supplementary Table S3.

4. Results

4.1. U-Pb zircon geochronology

Zircon grains separated for this study are prismatic crystals without obvious zoning (Fig. 4). They are 90–180 μm long with length to width ratios of 1:1–2:1 (Fig. 4). Fourteen analyses were carried out during the analytical session. The analysis results give variable Th (18–335 ppm) and U (168–729 ppm) contents with Th/U ratios ranging from 0.07 to 0.62 (Supplementary Table S1). All the fourteen analysis results are concordant with an age of 833 ± 3 Ma (95 % confidence interval, MSWD = 2.4). All 14 measurements give relatively consistent $^{207}Pb/^{206}Pb$ ages ranging from 790 ± 20 to 858 ± 17 with a weighted average age of 827 ± 8 Ma (2sigma; MSWD = 0.81) (Fig. 4).

4.2. Geochemical characteristics

Rocks from the mafic dykes in this study have low SiO_2 (48.38–53.61 wt%, recalculated to 100 % volatile and water free, the same below), high MgO (5.82–10.69 wt%), FeO^T (7.56–9.19 wt%), TiO_2 (1.35–1.89 wt%) and ($Na_2O + K_2O$) (5.10–7.10 wt%), as well as high Cr (167–622 ppm) and Ni (62–375 ppm). Major oxides such as TiO_2 and ($Na_2O + K_2O$), and trace elements such as Cr and Ni in the Nage samples from each dyke correlate well with their MgO (Fig. 5). The samples are generally plotted in the field of alkaline basalt in the TAS classification diagram (Fig. 6).

The samples exhibit OIB-like trace elemental patterns in the spider diagrams (Fig. 7a). They are rich in incompatible elements, and do not show significant Eu, Nb-Ta or Zr-Hf anomalies (Fig. 7a). Their chondrite-

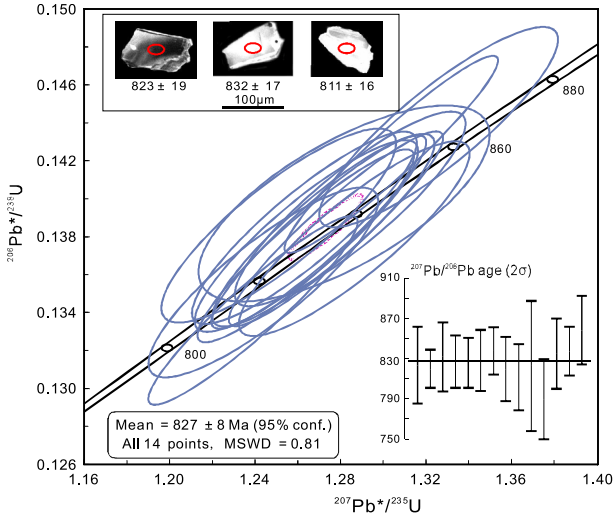

Fig. 4. Zircon U–Pb Concordia diagram with transmitted CL images of representative zircon grains from the Nage mafic dykes. Mean represent weighted mean $^{207}Pb/^{206}Pb$ age with 95 % confidence intervals (2σ). Red circles on zircon grain indicate the SIMS U–Pb dating positions. Age is presented as $^{207}Pb/^{206}Pb$ age (2σ). (For interpretation of the references to colour in this figure legend, the reader is referred to the web version of this article.)

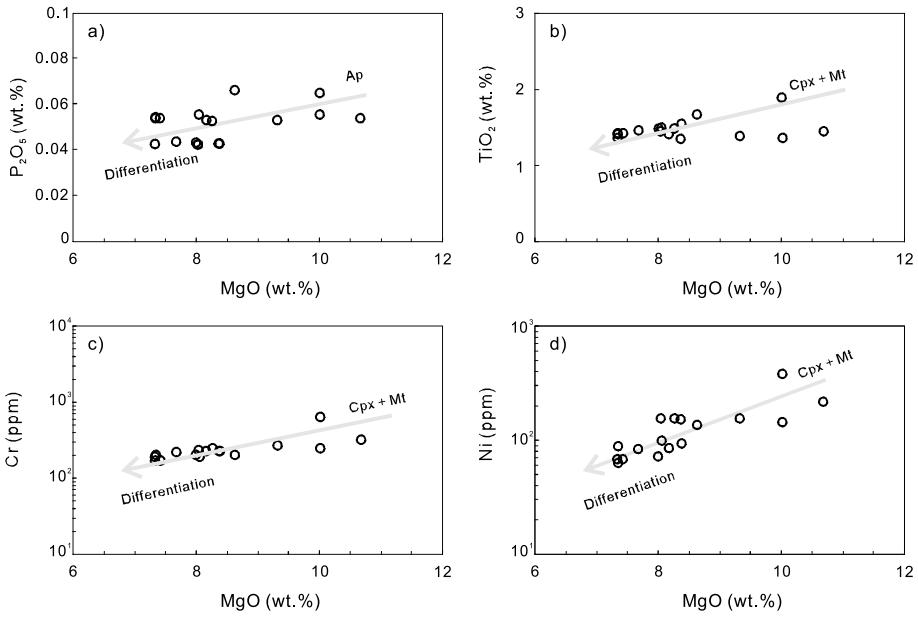

Fig. 5. Plots of a) P_2O_5 vs MgO, b) TiO_2 vs MgO, c) Cr vs MgO, and d) Ni vs MgO for the Nage mafic dykes. Ap = apatite, Cpx = clinopyroxene, Mt = magnetite.

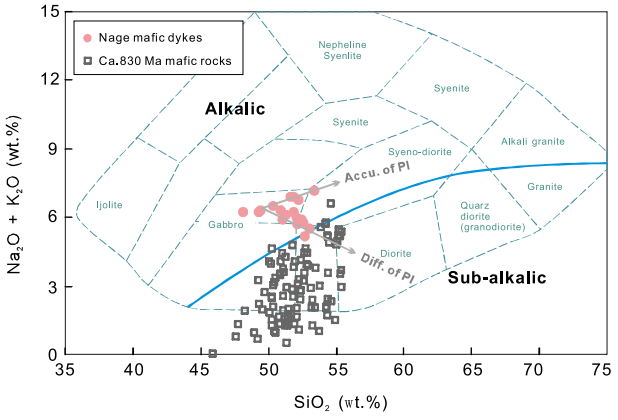

Fig. 6. Plots of (Na_2O + K_2O) vs SiO_2, modified after Cox et al. (1979), for classification of the Nage mafic dykes. Ca. 830 Ma mafic rocks in the Yangtze Block are from Ge et al. (2001), Wang et al. (2007a, 2019), Li et al. (2008a, 2016), Zhang et al. (2012, 2013b), Zhao and Zhou (2013), Yao et al. (2014a), Zhao and Asimow (2014), and Wu et al. (2022).

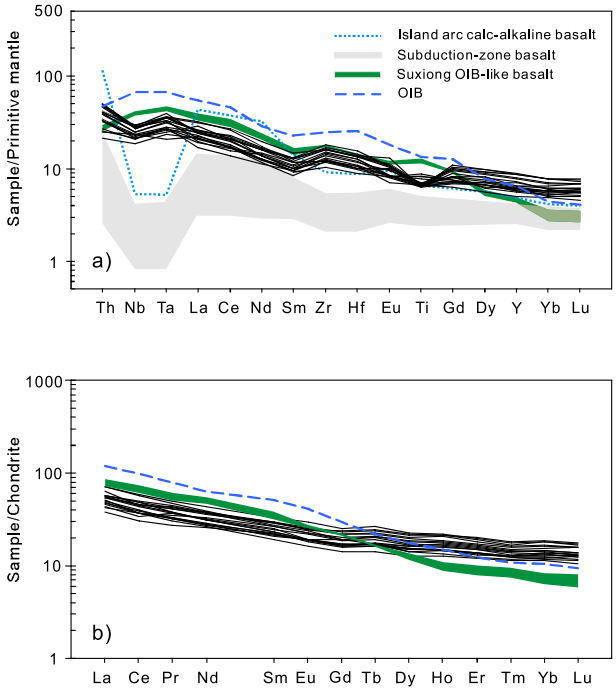

Fig. 7. A) primitive mantle-normalized incompatible trace element spider diagram for the nage mafic dykes with normalizing values fromSun and McDonough (1989), and b) chondrite-normalized REE patterns for the Nage mafic dykes with normalizing values from Boynton (1984). OIB and E-MORB data are from Sun and McDonough (1989); subduction-zone basalt is from Kelemen et al. (2003); island arc calc-alkaline basalt is from Tatsumi and Eggins (1995).

normalized REE patterns show LREE enrichment with $(La/Yb)_N$ ratios ranging from 2.76 to 4.97 with an exception of 7.58 (Fig. 7b). The above trace elements and REE compositions are similar to those of typical intraplate alkaline basaltic rocks identified in the world (Fig. 7) (Sun and McDonough, 1989).

Samples from the Nage dykes show slightly negative to positive $\varepsilon_{Nd}(T)$ values (-0.55 and 3.23) with $^{143}Nd/^{144}Nd_i$ values ranging from 0.511560 to 0.512374, and thus close to the field of asthenospheric mantle (Fig. 8).

5. Discussion

5.1. Effects of alteration

The long history of post-magmatic metamorphism and deformation has, more or less, modified the chemical composites of Neoproterozoic magmatic rocks exposed in the Yangtze Block. The samples collected from the Nage mafic dykes did not experience any metamorphism but have suffered various degrees of alteration/carbonatization regarding to their variable whole-rock LOI values (Supplementary Table S2) as well as the extensive albitization observed under microscope (Fig. 3). However, effects of alteration on major elements were insignificant regarding well correlations between some major oxides with MgO in the Nage samples (Fig. 5).In the following discussions, we will use the data of major oxides by corrected them to a dry magmatic system without volatiles and water. Elements including rare earth elements (REE), high-field strength elements (HFSE), and Zr in mafic magmatic rocks are

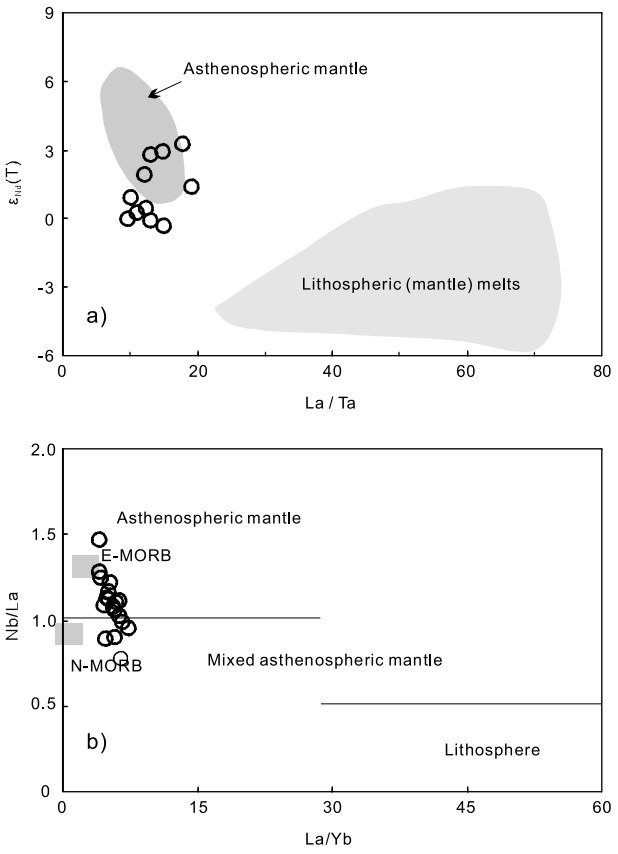

Fig. 8. A) plot of $\varepsilon_{Nd}(T)$ vs La/Ta. The fields of the asthenospheric and lithospheric melts are from Lawton and McMillan (1999); (b) Plot of La/Yb versus Nb/La (after Watson, 1993). Symbols as in Fig. 6.

generally immobile during alteration (e.g., Wood et al., 1979), which is confirmed by the parallel multi-elemental and REE patterns of the Nage dykes (Fig. 7) as well as the strongly correlations of HFSE (such as Nb and Th) and REE (such as Yb and Lu) with Zr (Supplementary Fig. S1). Therefore, they were not substantially modified by secondary alteration. In the following sections, only these immobile elements of relatively fresh samples are used for discussion.

5.2. Petrogenesis of the Nage mafic dykes

5.2.1. Differentiation processes and crustal contamination

Mafic dykes commonly inherited geochemical characters of their parental magma due to rapid cooling (Li et al., 2015). The Nage mafic dykes have variable SiO_2 (48.38–53.61 wt%) and MgO (5.82–10.69 wt %) contents as well as $\varepsilon_{Nd}(T)$ values (-0.55–3.23) (Supplementary Table S2-S3), suggesting the primary magma underwent varying degrees of fractional crystallization to produce their parental magmas with coherent variations. The variations of MgO and other major elements can be explained by various degrees of fractional crystallization in a deep magma chamber (Fig. 5), whereas the variable $\varepsilon_{Nd}(T)$ values may have inherited from a heterogeneous primary magma or resulted from crustal contamination. Therefore, influence of shallow-level magmatic processes on geochemical compositions of the mafic dykes must be evaluated before investigating characteristics of their mantle source.

Samples collected from the Nage mafic dykes show negative correlations for P_2O_5 against MgO (Fig. 5a), suggesting fractional crystallization of apatite, whereas their positive correlations for TiO_2, Cr and Ni against MgO may have resulted from fractionation of clinopyroxene and magnetite (Fig. 5b-d). The Nage mafic dykes were subjected to plagioclase fractionation and accumulation as indicated by the clear correlations between ($Na_2O + K_2O$) and SiO_2 (Fig. 6). Moreover, the Nage dyke samples show tightly linear regression lines in the plots of Si/K vs (2Na + Al)/K and Al/K vs (2Ca + Na)/K (Supplementary Fig. S2), suggesting that these major elements were mainly controlled by fractional crystallization of clinopyroxene and plagioclase (Russell and Nicholls, 1988). The above magma fractional crystallization is also supported by their large variable Nb/La ratio and Sm contents, but relatively constant La/Ta and Sm/Yb ratios (Figs. 9-10).

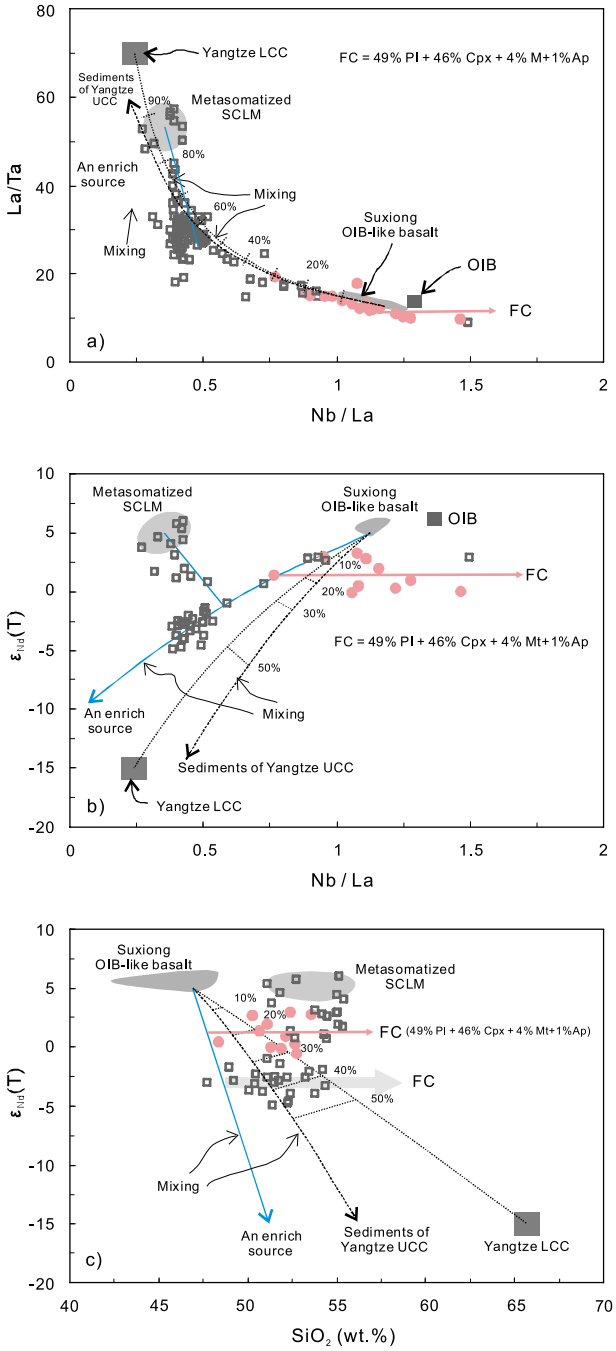

Fig. 9. Plots of a) La/Ta vs Nb/La, b) $\varepsilon_{Nd}(T)$ vs Nb/La, and c) $\varepsilon_{Nd}(T)$ vs SiO_2 for the Nage mafic dykes and published ca. 830 Ma mafic rocks in the Yangtze Block. OIB, Yangtze LCC, sediments of Yangtze UCC, and Suxiong OIB-like basalts data is from Sun and McDonough (1989), Gao et al. (1998, 1999), Li et al. (2002), Wang et al. (2013b) and reference therein. Partition coefficients used for the modeling are from GERM Partition Coefficients Database (https://earthref.org/). Cpx = clinopyroxene, Pl = plagioclase, Mt = magnetite, Ap = apatite. $\varepsilon_{Nd}(T)$ values of the Suxiong basalts were calculated using the age of 830 Ma. Symbols as in Fig. 6.

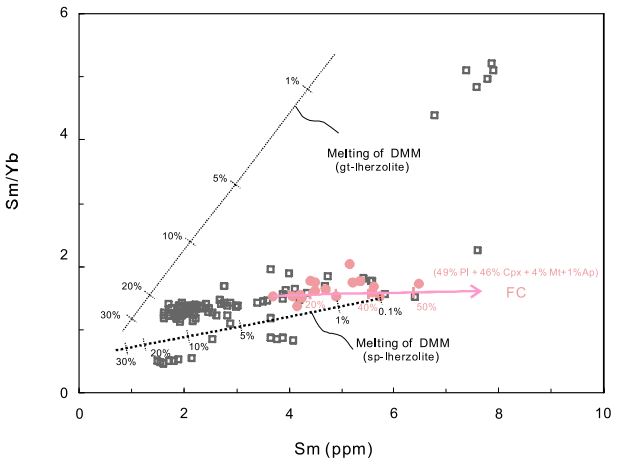

Fig. 10. Plots of Sm/Yb vs Sm for the Nage mafic dykes. OIB and LCC data is from Sun and McDonough (1989) and Gao et al. (1998), respectively. Melting curves are obtained using the non-modal batch melting equations of Shaw (1970). The assumed proportions of partial melting are 10–50 % Ol + 30–50 % Opx + 0–40 % Cpx + 0–20 % Gt for the garnet peridotite (Walter, 1998) and 20–35 % Ol + 20 % Opx + 20 % Cpx + 5–20 % Sp for the spinel peridotite (Kinzler, 1997). Depleted MORB mantle (DMM) is from Salters and Stracke (2004). The partition coefficients used for the modeling are from the GERM Partition Coefficients Database (https://earthref.org/). Cpx = clinopyroxene, Pl = plagioclase, Mt = magnetite, Ap = apatite, gt = garnet, sp = spinel. Symbols as in Fig. 6.

Samples from the Nage mafic dykes do not show strong Nb-Ta or Zr-Hf anomalies in the spider diagram (Fig. 7a), suggesting insignificant crustal contamination. Additionally, their $\varepsilon_{Nd}(T)$ values are not correlated with Nb/La ratios or SiO_2 contents (Fig. 9b-c), further supporting that fractional crystallization rather than crustal contamination controlled chemical compositions. Therefore, parental magmas of the Nage mafic dykes are likely the product of a heterogeneous primary magma which subsequently experienced variable fractional crystallization with negligible crustal contamination.

5.2.2. An OIB-like mantle source for the Nage dykes

The mafic dike samples in this study have slightly negative to positive $\varepsilon_{Nd}(T)$ values (-0.55 and 3.23) and are close to the field of asthenospheric mantle, suggesting that their primary magmas were derived from a depleted mantle source (Figs. 8-9). This is consistent with their relatively low La/Yb (4.10–7.38), La/Ta (9.71–19.22) and high Nb/La ratios (0.77–1.47) which are similar to those of basalts derived from depleted asthenospheric mantle but different from those produced by typical lithospheric mantle (Figs. 8 and 9). Their REE and trace element patterns are comparable with those of the alkaline basalts from the Suxiong Formation (810 Ma) at the western margin of the Yangtze Block, the latter is suggested to have been derived from an OIB-like, asthenospheric mantle (Fig. 7) (e.g., Li et al., 2002). Moreover, the Nage samples are all enriched in incompatible elements and LREE with negligible anomalies of Nb-Ta and Zr-Hf, which is obviously different from typical arc-related igneous rocks but comparable to intraplate OIB-like basaltic rocks (Fig. 7a) (e.g., Sun and McDonough, 1989). Therefore, the Nage mafic dykes show a much stronger affinity to OIB-like rocks derived from an asthenospheric mantle source than arc-related rocks, which are comparable to those of the 810 Ma alkaline Suxiong basalts in the Kangdian Rift, southwestern Yangtze Block (Li et al., 2002).

5.2.3. Involvement of plume-derived enriched components in their genesis

Variations in Nd isotopic compositions of the Nage mafic dykes were most likely inherited from their primary magma regarding negligible crustal contamination as discussed above. Modeling calculation based on Sm/Yb vs Sm for the Nage mafic dykes as presented in Fig. 10 suggests that primary magma for the Nage mafic dykes were probably generated from less than 5 degrees of partial melting of an depleted asthenospheric mantle (Fig. 10). The variations in $\varepsilon_{Nd}(T)$ values of the Nage mafic dykes were probably generated by the modifications of the enriched component to varying degrees (Fig. 8a and 9b-c). Small-degree partial melting of the depleted mantle with an enriched component has also been used to explain the genesis of other alkaline mafic rocks with OIB-like characters just like what we see in the Nage sample (e.g., Rogers et al., 1998). Therefore, an enriched component within their source region is required for the genesis of the Nage mafic dykes, which has produced the heterogeneous Nd isotopic signatures of their primary magma.

Such an enriched component is commonly suggested to be crustal-derived materials. A two-component mixing model is proposed to evaluate the possible involvement of crustal-derived materials into the genesis of the Nage mafic dykes. During this modeling calculation, the mantle source component is modeled using the 810 Ma alkaline Suxiong basalts (Li et al., 2002). The ranges for the Yangtze LCC and sediments of the Yangtze UC are from Gao et al. (1998, 1999), Wang et al. (2013b) and reference therein. Our two-component mixing modeling reveal that ~ 10–30 wt% crustal-derived materials from the Yangtze upper/lower continental crust are required to explain isotopic and elemental compositions of the Nage dykes, and ~ 20–90 wt% for other ca. 830 Ma mafic rocks in the Yangtze Block (Fig. 9), which is obviously impossible to achieve their geochemical feature regarding such a high proportion of crustal assimilation. Therefore, crustal material is not a reasonable candidate for the enriched component within their source region of those mafic rocks. Modeling in Fig. 9 also tells that depletions of Nb and Ta relative to La of the ca. 830 Ma mafic rocks in the Yangtze Block are due to the involvement of another enriched component rather than crustal materials. Enriched heterogeneities within melts produced by a depleted upper mantle have also been attributed to veins and dikes with enriched compositions (e.g., Niu et al., 2002). However, enriched compositions input by veins and dikes are unlikely to generate enriched signatures for such large volume of ca. 830 Ma mafic rocks widespread in central of South China (Fig. 1a and 9). Enriched features similar to that of the Nage dykes have been observed in many continental and oceanic intraplate alkaline rocks which were proposed to be genetically related to plume-derived enriched components from lower mantle even the core/mantle boundary that produce enriched heterogeneities within the asthenospheric mantle and then generate mafic rocks with an OIB-like enriched signature as we have noticed in the Nage mafic dykes (Hart, 1988). For example, an OIB-like magmatism with the involvement of a plume-derived enriched component in their genesis has been used to explain the origin of the alkaline basalts and mafic dykes identified in the modern East African Rift and Rio Grande Rift as well as the 260 Ma Panxi Rift and the 1720–1700 Ma Kangdian Rift (Pik et al., 1999; Xu et al., 2004; Chen et al., 2013; Burov and Gerya, 2014; Fan et al., 2020). Parental magmas of the Nage dykes have experienced varying degrees of fractional crystallization(Figs. 3-4 and 9-10), indicating that they are not suitable for the estimation of mantle potential temperature (Tp) to check if there exists a mantle plume or not (Herzberg and Asimow, 2008; Yang and Zhou, 2013). However, estimates based on the 823 ± 6 Ma Yiyang komatiitic basalts exposed nearby give Tp values much higher than that of ambient MORB but are closed to those of modern mantle plumes (Wang et al., 2007a; Putirka, 2008; Wu et al., 2018a). Therefore, a plume-derived enriched component is the best candidate for the enriched source required for the genesis of the Nage mafic dykes and other Ca.830 Ma mafic rocks in the Yangtze Block.

5.3. Tectonic implications

Origins and tectonic settings of the ca. 830 Ma mafic rocks in the Yangtze Block still remain controversial (Li et al., 1999; Ge et al., 2001; Wu et al., 2006, 2022; Wang et al., 2007a, 2019; Li et al., 2008b, 2013,2016; Zhao et al., 2011; Yin et al., 2013; Zhang et al., 2013b; Yao

et al., 2014a; Chen et al., 2015; Sun et al., 2018). They are suggested to have been produced in an intraplate (e.g., Wang et al., 2007a; Wu et al., 2018a) or an arc setting (Zhou et al., 2002a; Zhao et al., 2011, 2018; Zhao and Zhou, 2013; Zhao and Asimow, 2014). The Nage mafic dykes in this study show geochemical affinities of OIB-like basaltic rocks rather than arc-related rocks, and were more likely to have been derived from an asthenospheric mantle source in an extension environment that could be induced by back-arc extension, post-orogenic extension, or continental rifting (Mazzarini et al., 2004; Greentree et al., 2006).

Ca. 860–840 Ma bimodal volcanism has been identified along the southeastern margin of the Yangtze Block, which was closely followed by a quick lithospheric doming prior to 830 Ma (Li et al., 1991, 2008d; Zhao et al., 2011; Gao et al., 2011; Zhang and Zheng, 2013; Lyu et al., 2017; Zhang et al., 2019). A subsequent tectonic extension is suggested in the southeastern Yangtze Block (Zhang et al., 2008; Zheng et al., 2008; Zhao et al., 2011; Zhang and Zheng, 2013; Yao et al., 2014a, b; Chen et al., 2015). The bimodal magmatism followed by rapid lithospheric doming and the subsequent tectonic extension, are generally considered to represent a typical rift setting around the world (Pik et al., 1999; Xu et al., 2004; Burov and Gerya, 2014; Wang and Zhou, 2014; Fan et al., 2020). In addition, the 820–725 Ma Danzhou Group and its equivalents distributed from southwestern to southeastern of the Yangtze Block consists of slate, schist and greywacke interbedded with bimodal igneous rocks, has been suggested to be formed in a Neoproterozoic rift setting (Wang and Li, 2003; Wang et al., 2007a; Huang et al., 2009; Zhang et al., 2015; Zhao et al., 2018).

As described above, the ca.830 Ma Nage mafic dykes are alkaline in compositions, and do not show obvious negative Nb–Ta anomalies in the spider diagram which are commonly observed in calc-alkaline basaltic rocks in back-arc settings or post-orogenic basalts derived from previously-metasomatized lithospheric mantles (Saunders and Tarney, 1984). In addition, they were probably derived from a depleted asthenospheric mantle with an enriched component carried by a plume from lower mantle even the core/mantle boundary, genetically similar to the alkaline basalts and mafic dykes identified in plume-related rifts around the word, such as the modern East African Rift and Rio Grande Rift, the 260 Ma basalts and the 1720–1700 Ma from the Panxi-Kangdian Rift (Hart, 1988; Pik et al., 1999; Xu et al., 2004; Burov and Gerya, 2014; Fan et al., 2020). Some ca. 830 mafic rocks in southeastern margin of the Yangtze Block are emphasized to have "arc /boninite-like" geochemical signatures (e.g. Li et al. 2008b; Zhao and Asmow, 2014). However, "arc-like" geochemical signatures, such as Nb-Ta negative anomalies in the spider diagram, have also been identified in basaltic rock formed within intraplate rifting settings, probably formed by partial melting of slab melt-metasomatized SCLM (e.g. Li et al. 2008b). Moreover, Ca. 830–825 Ma high-MgO basalts with "boninite-like" geochemical signatures in the southern Yangtze Block have been recently suggested to be geochemically different from typical boninites but comparable to komatiitic basalts (Wu et al., 2018a). Furthermore, the above discussions on the characteristics of the source nature have demonstrated that a plume-derived component, rather than a crustal-derived material, was responsible for the depletions of Nb and Ta relative to La of the ca. 830–825 mafic rocks distributed from southern to southeastern of the Yangtze Block (Fig. 9a). Thus, these ca. 830–825 mafic rocks are likely generated in a plume related rifting system.

The ca. 830–825 Ma rift-related mafic rocks were closely followed by the ca. 820 Ma Tongde complex and associate picritic dykes (Li et al., 2010a), the ca. 820–810 Ma Bikou-Tiechuanshan continental flood basalts (e.g., Ling et al., 2003; Wang et al., 2008) and the ca. 810 Ma *syn*-rift Suxiong bimodal volcanic rocks (Li et al., 2002). This pattern of broadly concurrent intraplate mafic–ultramafic magmatisms in the Yangtze Block is comparable to those observed in plume-related large igneous provinces (Srivastava et al., 2022). Therefore, they were genetically linked to a mid-Neoproterozoic mantle plume which triggered partial melting of the asthenospheric and lithospheric mantles (Li et al., 2002, 2010b). In this scenario, the parental magmas of the ca. 830 Ma mafic rocks, including the Nage mafic dykes, were probably derived from upwelling of the mantle plume head, whereas the subsequent ca. 820–810 Ma mafic magmatism maybe the product of the plume tail. Most ca. 830 Ma mafic rocks experienced variable degrees of crustal contamination en route to their final emplacement (Wang et al., 2007a; Zhang et al., 2013b; Zhao and Zhou, 2013; Zhao and Asimow, 2014; Wu et al., 2022), whereas the younger mafic magmatism such as the ca. 820–810 Ma basalt from the Tiechuanshan and Suxiong Formations underwent negligible crustal contamination, which are consistent with experimental and numerical modeling results that plume tails commonly contaminate much less crustal components than plume heads (Hauri et al., 1994). In addition, the ca. 830–820 Ma mafic rocks, such as the Nage mafic dykes, Yiyang basalts and Bikou-Tiechuanshan continental flood basalts followed by that of ca. 810 Ma Suxiong basalt is consistent with the pattern that an OIB-like magma comes after a more enrich magma, which has been observed in many plume related magmatic actives, such as those in the Xiong'er Volcanic Province and the kangdian Rift and on the Hawaiian Islands (e.g., Wyllie, 1988; Peng et al., 2007; Fan et al., 2020). Therefore, both the tectonostratigraphic and geochemical evidence suggest that the ca. 830 Ma mafic rocks identified from southeastern to southeastern of the Yangtze Block were likely generated in a Neoproterozoic rift setting that was probably induced by a Neoproterozoic mantle plume beneath the Yangtze Block.

6. Conclusions

We report results of detailed geochronological and geochemical analyses on newly discovered alkaline mafic dykes at the Nage area in the southern Yangtze Block. SIMS zircon U-Pb age shows Nage dykes crystallized at 827 ± 8 Ma. Chemical compositions and isotopic characteristics of Nage alkaline mafic dykes are comparable to intraplate basaltic rocks but different from typical arc related volcanic rocks. They also show a close affinity to the alkaline basalts and mafic dykes identified in plume related rifting systems around the world. Our modeling shows that the primary magma for the Nage dykes was probable derived from an asthenospheric mantle with previously input of a plume-derived enriched component occurred within the source region, which subsequently experienced variable fractional crystallization with negligible crustal contamination to produce parental magmas of the Nage mafic dykes. Combined with preciously reported ca. 830 Ma mafic rocks in the Yangtze Block, our data suggest that they are likely generated in a plume-induced intraplate rift setting.

CRediT authorship contribution statement

Hong-Peng Fan: Data curation, Writing – original draft. **Jia-Xi Zhou:** Supervision, Project administration, Writing – review & editing. **Zhi-Long Huang:** Supervision, Project administration, Writing – review & editing. **Tao Wu:** Writing – review & editing. **Hao Zhang:** Writing – review & editing.

Declaration of Competing Interest

The authors declare that they have no known competing financial interests or personal relationships that could have appeared to influence the work reported in this paper.

Data availability

Data will be made available on request.

Acknowledgements

The paper has benefited from English polishing and constructive comments of the Prof. J.-H. Zhao, Prof. X.-P. Xia, and two anonymous reviewers. This research was financially supported by the National

Natural Science Foundation of China (Nos. U1812402, 41763003 and 42072069), the State Key Program of National Natural Science Foundation of China (No. 92162218), CAS "Light of West China" Program, the Science and Technology Foundation of Guizhou Province (2012–2334), Guizhou Provincial Science and Technology Support Program (QKHZC[2019]2859), and a Research Startup Project (YJRC4201804) of Yunnan University to J.-X. Zhou.

Appendix A. Supplementary material

Supplementary data to this article can be found online at https://doi.org/10.1016/j.precamres.2023.107032.

References

Boynton, W.V., 1984. Geochemistry of the rare earth elements: meteorite studies. In: Henderson, P. (Ed.), Rare Earth Element Geochemistry. Elsevier, pp. 63–114.
Burov, E., Gerya, T., 2014. Asymmetric three-dimensional topography over mantle plumes. Nature 513, 85–89.
Chen, Z.H., Xing, G.F., Guo, K.Y., Dong, Y.G., Chen, R., Zeng, Y., Li, L.M., He, Z.Y., Zhao, L., 2009. Petrogenesis keratophyres in the Pingshui Group, Zhejiang: constraints from zircon U-Pb ages and Hf isotopes. Chin. Sci. Bull. 54, 1570–1578.
Chen, W.T., Zhou, M.F., Zhao, X.F., 2013. Late Paleoproterozoic sedimentary and mafic rocks in the Hekou area, SW China: Implication for the reconstruction of the Yangtze Block in Columbia. Precambr. Res. 231, 61–77.
Chen, W.T., Sun, W.H., Wang, W., Zhao, J.H., Zhou, M.F., 2014. "Grenvillian" intra-plate mafic magmatism in the southwestern Yangtze Block, SW China. Precambr. Res. 242, 138–153.
Chen, Q., Sun, M., Long, X.P., Yuan, C., 2015. Petrogenesis of Neoproterozoic adakitic tonalites and high-k granites in the eastern songpan-ganze fold belt and implications for the tectonic evolution of the western Yangtze Block. Precambr. Res. 270, 181–203.
Chen, X., Wang, X.L., Wang, D., Shu, X.J., 2018. Contrasting mantle-crust melting processes within orogenic belts: Implications from two episodes of mafc magmatism in the western segment of the Neoproterozoic Jiangnan Orogen in South China. Precambr. Res. 309, 123–137.
Cox, K.G., Bell, J.D., Pankhurst, R.J., 1979. The Interpretation of Igneous Rocks. Allen and Unwin, London, UK, p. 450.
Cui, X., Wang, J., Wang, X.-C., Wilde, S.A., Ren, G., Li, S., Deng, Q.I., Ren, F., Liu, J., 2021. Early crustal evolution of the Yangtze Block: Constraints from zircon U-Pb-Hf isotope systematics of 3.1–1.9 Ga granitoids in the Cuoke Complex, SW China. Precambr. Res. 357, 106155.
Du, L.L., Guo, J.H., Nutman, A.P., Wyman, D., Geng, Y.S., Yang, C.H., Liu, F.L., Liu, L.D., Zhou, X.W., 2014. Implications for Rodinia reconstructions for the initiation of Neoproterozoic subduction at ~860 Ma on the western margin of the Yangtze Block: Evidence from the Guandaoshan Pluton. Lithos 196, 67–82.
Fan, H.P., Zhu, W.G., Li, Z.X., 2020. Paleo- to Mesoproterozoic magmatic and tectonic evolution of the southwestern Yangtze Block, south China: New constraints from ca. 1.7–1.5 Ga mafic rocks in the Huili-Dongchuan area. Gandwana Res. 87, 248–262.
Gao, L.Z., Dai, C.G., Ding, X.Z., Wang, M., Liu, Y.X., Wang, X.H., Chen, J.S., 2011. SHRIMP U-Pb dating of intrusive alaskite in the Fanjingshan Group and alaskite basal conglomerates: constraints on the deposition of the Xiajiang Group. Geol. China 38, 1413–1420 in Chinese with English abstract.
Gao, S., Luo, T.C., Zhang, B.R., Zhang, H.F., Han, Y.W., Zhao, Z.D., Hu, Y.K., 1998. Chemical composition of the continental crust as revealed by studies in East China. Geochim. Cosmochim. Acta 62, 1959–1975.
Gao, S., Ling, W., Qiu, Y., Lian, Z., Hartmann, G., Simon, K., 1999. Contrasting geochemical and Sm-Nd isotopic compositions of Archean metasediments from the Kongling high-grade terrain of the Yangtze craton: evidence for cratonic evolution and redistribution of REE during crustal anatexis. Geochim. Cosmochim. Acta 63, 2071–2088.
Ge, W.C., Li, X.H., Liang, X.R., Wang, R.C., Li, Z.X., Zhou, H.W., 2001. Geochemical and geological implications of mafic-ultramafic rocks with age of 825 Ma in Yuanbaoshan-Baotan area of northern Guangxi. Geochimica 30 (2), 123–130 in Chinese with English abstract.
Geng, Y., Yang, C., Du, L., Wang, X., Ren, L., Zhou, X., 2007. Chronology and tectonic environment of the Tianbaoshan formation: new evidence from zircon SHRIMP U-Pb age and geochemistry. Geol. Rev. 53, 556–563 in Chinese with English abstract.
Greentree, M.R., Li, Z.X., Li, X.H., Wu, H., 2006. Late Mesoproterozoic to earliest Neoproterozoic basin record of the Sibao orogenesis in western South China and relationship to the assembly of Rodinia. Precambr. Res. 151, 79–100.
Hart, S.R., 1988. Heterogeneous mantle domains: signatures, genesis and mixing chronologies. Earth Planet. Sci. Lett. 90, 273–296.
Hauri, E.H., Whitehead, J.A., Hart, S.R., 1994. Fluid dynamic and geochemical aspects of entrainment in mantle plumes. J. Geophys. Res. 99, 275–300.
Herzberg, C., Asimow, P.D., 2008. Petrology of some oceanic island basalts: PRIMELT2. XLS software for primary magma calculation. Geochem. Geophys. Geosyst. 8, Q09001.
Huang, X.L., Xu, X.G., Li, X.H., Li, W.X., Lan, J.B., Zhang, H.H., Liu, Y.S., Wang, Y.B., Li, H.Y., Luo, Z.Y., Yang, Q.J., 2008. Petrogenesis and tectonic implications of Neoproterozoic highly fractionated A-type granites from Mianning, South China. Precambr. Res. 165, 190–204.
Huang, X.L., Xu, Y.G., Lan, J.B., Yang, Q.J., Luo, Z.Y., 2009. Neoproterozoic adakitic rocks from Mopanshan in the western Yangtze Craton: partial melts of a thickened lower crust. Lithos 112, 367–381.
Kelemen, P., Hanghøj, K., Greene, A., 2003. One view of the geochemistry of subduction-related magmatic arcs, with an emphasis on primitive andesite and lower crust. Treatise on Geochem. 3, 593–659.
Kinzler, R.J., 1997. Melting of mantle peridotite at pressures approaching the spinel to garnet transition: application to mid-ocean ridge basalt petrogenesis. J. Geophys. Res. 102, 853–874.
Lawton, T.F., McMillan, N.J., 1999. Arc abandonment as a cause for passive continental rifting: comparison of the Jurassic Mexican Borderland rift and the Cenozoic Rio Grande rift. Geology 27, 779–782.
Li, J., 1991. Characteristics of Jinning-Chengjiang magmatic rocks and plate tectonic movements. In: Liu, H. (Ed.), The Sinian System in China. Science Press, Beijing, pp. 220–300.
Li, C., Arndt, N.T., Tang, Q.Y., Ripley, E.M., 2015. Trace element indiscrimination diagrams. Lithos 232, 76–83.
Li, Z.X., Li, X.H., Kinny, P.D., Wang, J., 1999. The breakup of Rodinia: did it start with a mantle plume beneath South China? Earth Planet. Sci. Lett. 173, 171–181.
Li, Z.X., Bogdanova, S.V., Collins, A.S., Davidson, A., De Waele, B., Ernst, R.E., Fitzsimons, I.C.W., Fuck, R.A., Gladkochub, D.P., Jacobs, J., Karlstrom, K.E., Lu, S., Natapov, L.M., Pease, V., Pisarevsky, S.A., Thrane, K., Vernikovsky, V., 2008a. Assembly, configuration, and break-up history of Rodinia: a synthesis. Precambr. Res. 160, 179–210.
Li, Z.X., Chen, H.L., Li, X.H., Zhang, F.Q., 2014. Tectonics of South China-Interpreting the rock record. Science Press, Beijing, p. 144.
Li, X.H., Li, Z.X., Zhou, H.W., Liu, Y., Kinny, P.D., 2002. U-Pb zircon geochronology geochemistry and Nd isotopic study of Neoproterozoic bimodal volcanic rocks in the Kangdian Rift of South China: implications for the initial rifting of Rodinia. Precambr. Res. 113, 135–154.
Li, X.H., Li, Z.X., Ge, W.C., Zhou, H.W., Li, W.X., Liu, Y., Wingate, M.T.D., 2003. Neoproterozoic granitoids in South China: crustal melting above a mantle plume at ca. 825 Ma? Precambr. Res. 122, 45–83.
Li, W.X., Li, X.H., Li, Z.X., 2008b. Middle Neoproterozoic syn-rifting volcanic rocks in Guangfeng, South China: petrogenesis and tectonic significance. Geol. Mag. 145, 475–489.
Li, W.X., Li, X.H., Li, Z.X., Lou, F.S., 2008c. Obduction-type granites within the NE Jiangxi Ophiolite: Implications for the final amalgamation between the Yangtze and Cathaysia Blocks. Gondw. Res. 13, 288–301.
Li, X.H., Li, W.X., Li, Z.X., Liu, Y., 2008d. 850–790Ma bimodal volcanic and intrusive rocks in northern Zhejiang, South China: a major episode of continental rift magmatism during the breakup of Rodinia. Lithos 102, 341–357.
Li, X.H., Liu, Y., Li, Q.L., Guo, C.H., Chamberlain, K.R., 2009. Precise determination of Phanerozoic zircon Pb/Pb age by multi-collector SIMS without external standardization. Geochem. Geophys. Geosyst. 10, Q04010. https://doi.org/10.1029/2009GC002400.
Li, X.H., Zhu, W.G., Zhong, H., Wang, X.C., He, D.F., Bai, Z.J., Liu, F., 2010a. The Tongde picritic dikes in the western Yangtze block: evidence for ca. 800-ma mantle plume magmatism in south china during the breakup of Rodinia. J. Geol. 118, 509–522.
Li, X.H., Li, W.X., Li, Q.L., Wang, X.C., Liu, Y., Yang, Y.H., 2010b. Petrogenesis and tectonic significance of the 850 Ma Gangbian alkaline complex in South China: evidence from in situ zircon U-Pb dating, Hf–O isotopes and whole-rock geochemistry. Lithos 114, 1–15.
Li, W.X., Li, X.H., Li, Z.X., 2010c. Ca. 850 Ma bimodal volcanic rocks in northeastern Jiangxi Province, South China: initial extension during the breakup of Rodinia? Am. J. Sci. 310, 951–980.
Li, L.M., Lin, S.F., Xing, G.F., Davis, D.W., Davis, W.J., Xiao, W.J., Yin, C.Q., 2013. Geochronology and geochemistry of volcanic rocks from the Shaojiwa Formation and Xingzi Group, Lushan area, SE China: implications for Neoproterozoic back-arc basin in the Yangtze Block. Precambr. Res. 238, 1–17.
Li, L.M., Lin, S.F., Xing, G.F., Davis, D.W., Jiang, Y., Davis, W., Zhang, Y.J., 2016. Ca. 830 Ma back-arc type volcanic rocks in the eastern part of the Jiangnan orogen: Implications for the Neoproterozoic tectonic evolution of South China Block. Precambr. Res. 275, 209–224.
Li, Z.X., Zhang, L., Powell, C.M., 1995. South China in Rodinia: part of the missing link between Australi-East Antarctica and Laurentia? Geology 23, 407–410.
Li, Z.X., Wartho, J.A., Occhipinti, S., Zhang, C.L., Li, X.H., Wang, J., Bao, C.M., 2007. Early history of the eastern Sibao orogen (South China) during the assembly of Rodinia: new $^{40}Ar/^{39}Ar$ dating and U-Pb SHRIMP detrital zircon provenance constraints. Precambr. Res. 159, 74–94.
Li, Y., Yin, C.Q., Lin, S.F., Zhang, J., Gao, P., Qian, J.H., Xia, Y.F., Liu, J.G., 2021. Geochronology and geochemistry of bimodal volcanic rocks from the western Jiangnan Orogenic Belt: Petrogenesis, source nature and tectonic implication. Precambr. Res. 359, 106218.
Lin, G.C., Li, X.H., Li, W.X., 2007. SHRIMP U-Pb zircon age, geochemistry and Nd–Hf isotope of Neoproterozoic mafic dyke swarms in western Sichuan: petrogenesis and tectonic significance. Science in China Series D 50, 1–16.
Lin, M.S., Peng, S.B., Jiang, X.F., Polat, A., Kusky, T., Wang, Q., Deng, H., 2016. Geochemistry, petrogenesis and tectonic setting of Neoproterozoic mafic–ultramafic rocks from the western Jiangnan orogen, South China. Gondw. Res. 35, 338–356.
Ling, W., Gao, S., Zhang, B., Li, H., Liu, Y., Cheng, J., 2003. Neoproterozoic tectonic evolution of the northwestern Yangtze craton South China: implications for amalgamation and break-up of the Rodinia supercontinent. Precambr. Res. 122, 111–140.

Lu, G.M., Spencer, C.J., Deng, X., Tian, Y., Huang, B., Jiang, Y.D., Wang, W., 2022. Mesoproterozoic magmatism redefines the tectonics and paleogeography of the SW Yangtze Block. China. Precambr. Res. 370, 106558.
Lyu, P.L., Li, W.X., Wang, X.C., Pang, C.J., Cheng, J.X., Li, X.H., 2017. Initial breakup of supercontinent Rodinia as recorded by ca 860–840 Ma bimodal volcanism along the southeastern margin of the Yangtze Block, South China. Precambr. Res. 296, 148–167.
Mazzarini, F., Corti, G., Manetti, P., Innocenti, F., 2004. Strain rate and bimodal volcanism in the continental rift: Debre Zeyt volcanic field, northern MER, Ethiopia. J. Afr. Earth Sc. 39, 415–420.
Meert, J.G., Santosh, M., 2017. The Columbia supercontinent revisited. Gondw. Res. 50, 67–83.
Mou, C.L., Lin, S.L., Yu, Q., 2003. The U-Pb ages of the volcanic rock of the Tianbaoshan formation, Huili, Sichuan province. J. Stratigr. 27, 216–219 in Chinese with English abstract.
Niu, Y., Regelous, M., Wendt, I.J., Batiza, R., O'Hara, M.J., 2002. Geochemistry of near-EPR seamounts: importance of source vs. process and the origin of enriched mantle component. Earth Planet. Sci. Lett. 199, 327–345.
Peng, P., Zhai, M.G., Guo, J.H., Kusky, T., Zhao, T.P., 2007. Nature of mantle source contributions and crystal differentiation in the petrogenesis of the 1.78 Ga mafic dykes in the central North China craton. Gondw. Res. 12, 29–46.
Pik, R., Deniel, C., Coulon, C., Yirgu, G., Marty, B., 1999. Isotopic and trace element signatures of Ethiopian flood basalts: evidence for plume-lithosphere interaction. Geochim. Cosmochim. Acta 63, 2263–2279.
Putirka, K., 2008. Excess temperatures at ocean islands: Implications for mantle layering and convection. Geology 36, 283–286.
Qi, L., Hu, J., Grégoire, D.C., 2000. Determination of trace elements in granites by inductively coupled plasma mass spectrometry. Talanta 51, 507–513.
Raczek, I., Jochum, K.P., Hofmann, A.W., 2003. Neodymium and strontium isotope data for USGS reference materials BCR-1, BCR-2, BHVO-1, BHVO-2, AGV-1, AGV-2, GSP-1, GSP-2 and eight MPI-DING reference glasses. Geostand. Newslett. 27 (2), 173–179.
Rogers, N.W., James, D., Kelley, S.P., DeMulder, M., 1998. The generation of potassic lavas from the eastern Virunga province. Rwanda. J. Petrol. 39, 1223–1247.
Russell, J.K., Nicholls, J., 1988. Analysis of petrologic hypotheses with Pearce element ratios. Contrib. Miner. Petrol. 99, 25–35.
Salters, V., Stracke, A., 2004. Composition of the depleted mantle. Geochem. Geophys. Geosyst. 5 https://doi.org/10.1029/2003GC000597.
Saunders, A.D., Tarney, J., 1984. Geochemical characteristics of basaltic volcanism within back-arc basins. Geological Society. London (Special Publications) 16, 59–76.
Shaw, D.M., 1970. Trace element fractionation during anatexis. Geochim. Cosmochim. Acta 34, 237–243.
Srivastava, R.K., Ernst, R.E., Buchan, K.L., de Kock, M., 2022. An overview of the plumbing systems of large igneous provinces and their significance. Geol. Soc. Lond. Spec. Publ. 518, 1–16.
Sun, S.S., McDonough, W.F., 1989. Chemical and isotopic systematics of oceanic basalts: implications for mantle composition and processes. In: Saunders, A.D., Norry, M.J. (Eds.), Magmatism in the Ocean Basins. Geological Society, London Special Publications 42, pp. 313–345.
Sun, Z.M., Wang, X.L., Qi, L., Zhang, F.F., Wang, D., Li, J.Y., Yu, M.G., Shu, X.J., 2018. Formation of the Neoproterozoic ophiolites in southern China: new constraints from trace element and PGE geochemistry and Os isotopes. Precambr. Res. 309, 88–101.
Tatsumi, Y., Eggins, S.M., 1995. Subduction Zone Magmatism. Blackwell Science, Cambridge, Boston, p. 211.
Walter, M.J., 1998. Melting of Garnet Peridotite and the Origin of Komatiite and depleted Lithosphere. J. Petrol. 39, 29–60.
Wang, J., Li, Z.X., 2003. History of Neoproterozoic rift basins in South China: implications for Rodinia break-up. Precambr. Res. 122, 141–158.
Wang, X.C., Li, X.H., Li, W.X., Li, Z.X., 2007a. Ca. 825 Ma komatiitic basalts in South China, first evidence for>1500°C mantle melts by a Rodinia mantle plume. Geology 35, 1103–1106.
Wang, X.C., Li, X.H., Li, W.X., Li, Z.X., 2008. The Bikou basalts in the northwestern Yangtze block, South China: remnants of 820–810 Ma continental flood basalts? Geol. Soc. Am. Bull. 120 https://doi.org/10.1130/B26310.1.
Wang, X.L., Zhou, J.C., Qiu, J.S., Zhang, W.L., Liu, X.M., Zhang, G.L., 2006. LA-ICP-MS U-Pb zircon geochronology of the Neoproterozoic igneous rocks from Northern Guangxi, South China: Implications for tectonic evolution. Precambr. Res. 145, 111–130.
Wang, X.L., Zhou, J.C., Griffin, W.L., Wang, R.C., Qiu, J.S., O'Reilly, S.Y., Xu, X., Liu, X. M., Zhang, G.L., 2007b. Detrital zircon geochronology of Precambrian basement sequences in the jiangnan orogen: dating the assembly of the yangtze and cathaysia blocks. Precambr. Res. 159, 117–131.
Wang, X.L., Shu, L.S., Xing, G.F., Zhou, J.C., Tang, M., Shu, X.J., Qi, L., Hu, Y.H., 2012b. Post-orogenic extension in the eastern part of the Jiangnan Orogen: evidence from ca 800 760 Ma volcanic rocks. Precambr. Res. 222–223, 404–423.
Wang, Q., Wyman, D.A., Li, Z.X., Bao, Z.W., Zhao, Z.H., Wang, Y.X., Jian, P., Yang, Y.H., Chen, L.L., 2010. Petrology, geochronology and geochemistry of ca. 780 Ma A-type granites in South China: petrogenesis and implications for crustal growth during the breakup of the supercontinent Rodinia. Precambr. Res. 178, 185–208.
Wang, Y.J., Zhang, A.M., Cawood, P.A., Fan, W.M., Xu, J.F., Zhang, G.W., Zhang, Y.Z., 2013a. Geochronological, geochemical and Nd–Hf–Os isotopic fingerprinting of an early Neoproterozoic arc–back-arc system in South China and its accretionary assembly along the margin of Rodinia. Precambr. Res. 231, 343–371.
Wang, Y.J., Zhang, A.M., Fan, W.M., Zhang, Y.Z., Zhang, Y.H., 2013b. Origin of paleosubduction-modified mantle for Silurian gabbro in the Cathaysia Block: geochronological and geochemical evidence. Lithos 160–161, 37–54.
Wang, W., Zhou, M.F., Yan, D.P., Li, J.W., 2012a. Depositional age, provenance, and tectonic setting of the Neoproterozoic Sibao Group, southeastern Yangtze Block, South China. Precambr. Res. 192, 107–124.
Wang, Z., Zhou, B., Guo, Y., Yang, B., Liao, Z., Wang, S., 2012c. Geochemistry and zircon U-Pb dating of Tangtang granite in the western margin of the Yangtze Platform. Acta Petrol. Mineral. 31, 652–662 in Chinese with English abstract.
Wang, X.L., Zhou, J.C., Griffin, W.L., Zhao, G., Yu, J.H., Qiu, J.S., Zhang, Y.J., Xing, G.F., 2014. Geochemical zonation across a Neoproterozoic orogenic belt: isotopic evidence from granitoids and metasedimentary rocks of the Jiangnan orogen, China. Precambr. Res. 242, 154–171.
Wang, Y.J., Zhou, Y.Z., Cai, Y.F., Liu, H.C., Zhang, Y.Z., Fan, W.M., 2016. Geochronological and geochemical constraints on the petrogenesis of the Ailaoshan granitic and migmatite rocks and its implications on Neoproterozoic subduction along the SW Yangtze Block. Precambr. Res. 283, 106–124.
Wang, Y.J., Zhang, Y.Z., Cawood, P.A., Zhou, Y.Z., Zhang, F.F., Yang, X., Cui, X., 2019. Early Neoproterozoic assembly and subsequent rifting in South China: revealed from mafic and ultramafic rocks, central Jiangnan Orogen. Precambr. Res. 331, 105367.
Wang, W., Zhou, M.F., 2014. Provenance and tectonic setting of the Paleo- to Mesoproterozoic Dongchuan Group in the southwestern Yangtze Block, South China: implication for the breakup of the supercontinent Columbia. Tectonophysics 610, 110–127.
Watson, S., 1993. Rare earth element inversions and percolation models for Hawaii. J. Petrol. 34, 763–783.
Wood, D.A., Joron, J.L., Treuil, M., 1979. A re-appraisal of the use of trace elements to classify and discriminate between magma series erupted in different tectonic settings. Earth Planet. Sci. Lett. 45, 326–336.
Wu, T., Wang, X.C., Li, W.X., Wilde, S.A., Tian, L., Pang, C.J., Li, J., 2018a. The 825 Ma Yiyang high–MgO basalts of central South China: Insights from Os–Hf–Nd data. Chem. Geol. 502, 107–121.
Wu, T., Zhou, J.X., Wang, X.C., Li, W.X., Wilde, S.A., Sun, H.R., Wang, J.S., Li, Z., 2018b. Identification of ca. 850 Ma high-temperature strongly peraluminous granitoids in southeastern Guizhou Province, South China: a result of early extension along the southern margin of the Yangtze Block. Precambr. Res. 308, 18–34.
Wu, T., Wang, X.C., Wilde, S.A., Li, Q.L., Pang, C.J., Zhou, J.X., 2022. Decoupling of isotopes between magmatic zircons and their mafic host rocks: a case study from the ca. 830 Ma Jiabang dolerite, South China. Precambr. Res. 369, 106519.
Wu, R.X., Zheng, Y.F., Wu, Y.B., Zhao, Z.F., Zhang, S.B., Liu, X.M., Wu, F.Y., 2006. Reworking of juvenile crust: element and isotope evidence from Neoproterozoic granodiorite in South China. Precambr. Res. 146, 179–212.
Wyllie, P.J., 1988. Magma genesis, plate tectonics and chemical differentiation of the Earth. Rev. Geophys. 26, 370–404.
Xu, Y.G., He, B., Chung, S.L., Menzies, M.A., Frey, F.A., 2004. Geologic, geochemical, and geophysical consequences of plume involvement in the Emeishan flood-basalt province. Geology 32, 917–920.
Yang, C., Li, X.H., Wang, X.C., Lan, Z., 2015. Mid-Neoproterozoic angular unconformity in the Yangtze Block revisited: insights from detrital zircon U-Pb age and Hf–O isotopes. Precambr. Res. 266, 165–178.
Yang, Z.F., Zhou, J.H., 2013. Can we identify source lithology of basalt? Sci. Rep. 3, 1856.
Yang, Y.J., Zhu, W.G., Bai, Z.J., Zhong, H., Ye, X.T., Fan, H.P., 2017. Petrogenesis and tectonic implications of the Neoproterozoic Datian mafic–ultramafic dykes in the Panzhihua area, western Yangtze Block, SW China. Int. J. Earth Sci. 10, 185–213.
Yao, J.L., Shu, L.S., Santosh, M., 2014a. Neoproterozoic arc-trench system and breakup of the South China Craton: constraints from N-MORB type and arc related mafic rocks, and anorogenic granite in the Jiangnan orogenic belt. Precambr. Res. 247, 187–207.
Yao, J.L., Shu, L.S., Santosh, M., Zhao, G.C., 2014b. Neoproterozoicarc-related mafic-ultramafic rocks and syn-collision granite from the western segment of the Jiangnan Orogen, South China: constraints on the Neoproterozoic assembly of the Yangtze and Cathaysia Blocks. Precambr. Res. 243, 39–62.
Yao, J.L., Cawood, P.A., Shu, L.S., Zhao, G.C., 2019. Jiangnan Orogen, South China: A ~970–820 Ma Rodinia margin accretionary belt. Earth Sci. Rev. 196, 102872.
Ye, M.F., Li, X.H., Li, W.X., Liu, Y., Li, Z.X., 2007. SHRIMP zircon U-Pb geochronological and whole-rock geochemical evidence for an early Neoproterozoic Sibaoan magmatic arc along the southeastern margin of the Yangtze Block. Gondw. Res. 12, 144–156.
Yin, C.Q., Lin, S.F., Davis, D.W., Xing, G.F., Davis, W.J., Cheng, G.H., Xiao, W.J., Li, L.M., 2013. Tectonic evolution of the southeastern margin of the Yangtze Block: constraints from SHRIMP U-Pb and LA-ICP-MS Hf isotopic studies of zircon from the eastern Jiangnan Orogenic Belt and implications for the tectonic interpretation of South China. Precambr. Res. 236, 145–156.
Zhang, C.H., Gao, L.Z., Wu, Z.J., Shi, X.Y., Yan, Q.R., Li, D.J., 2007. SHRIMP U-Pb zircon age of tuff from the Kunyang group in central Yunnan: evidence for Grenvillian orogeny in south China. Chin. Sci. Bull. 52, 1517–1525.
Zhang, C.L., Li, H.K., Santosh, M., 2013a. Revisiting the tectonic evolution of South China: interaction between the Rodinia superplume and plate subduction? Terra Nova 25, 212–220.
Zhang, C.L., Santosh, M., Zou, H.B., Li, H.K., Hung, W.C., 2013b. The Fuchuan ophiolite in Jiangnan Orogen: geochemistry, zircon U-Pb geochronology, Hf isotope and implications for the Neoproterozoic assembly of South China. Lithos 179, 263–274.
Zhang, Y.Z., Wang, Y.J., Geng, H.Y., Zhang, Y.H., Fan, W.M., Zhong, H., 2013c. Early Neoproterozoic (~850Ma) back-arc basin in the Central Jiangnan Orogen (Eastern South China): geochronological and petrogenetic constraints from meta-basalts. Precambr. Res. 231, 325–342.

Zhang, Y.Z., Wang, Y.J., Zhang, Y.H., Zhang, A.M., 2015. Neoproterozoic assembly of the Yangtze and Cathaysia blocks: evidence from the Cangshuipu Group and associated rocks along the Central Jiangnan Orogen, South China. Precambr. Res. 269, 18–30.
Zhang, F.F., Wang, X.L., Wang, D., Yu, J.H., Zhou, X.H., Sun, Z.M., 2017. Neoproterozoic back arc basin on the southeastern margin of the Yangtze block during Rodinia assembly: New evidence from provenance of detrital zircons and geochemistry of mafic rocks. Geol. Soc. Am. Bull. 129, 904–919.
Zhang, J.W., Ye, T.P., Dai, Y.R., Chen, J.S., Zhang, H., Dai, C.G., Yuan, C.H., Jiang, K., 2019. Provenance and tectonic setting transition as recorded in the Neoproterozoic strata, western Jiangnan Orogen: implications for South China within Rodinia. Geosci. Front. 10, 1823–1839.
Zhang, S.B., Zheng, Y.F., Zhao, Z.F., Wu, Y.B., Yuan, H.L., Wu, F.Y., 2008. Neoproterozoic anatexis of Archean lithosphere: geochemical evidence from felsic to mafic intrusions at Xiaofeng in the Yangtze Gorge, South China. Precambr. Res. 163, 210–238.
Zhang, S.B., Zheng, Y.F., 2013. Formation and evolution of Precambrian continental lithosphere in South China. Gondw. Res. 23, 1241–1260.
Zhang, S.B., Wu, R.X., Zheng, Y.F., 2012. Neoproterozoic continental accretion in South China: geochemical evidence from the Fuchuan ophiolite in the Jiangnan orogen. Precambr. Res. 220–221, 45–64.
Zhao, J.H., Asimow, P.D., 2014. Neoproterozoic boninite-series rocks in South China: a depleted mantle source modified by sediment-derived melt. Chem. Geol. 388, 98–111.
Zhao, G.C., Cawood, P.A., 2012. Precambrian geology of China: Precambr. Res. 222, 13–54.
Zhao, G.C., Cawood, P.A., Wilde, S.A., Sun, M., 2002. Review of global 2.1–1.8 Ga orogens: implications for a pre-Rodinia supercontinent. Earth Sci. Rev. 59, 125–162.
Zhao, J.H., Wang, W., 2021. Precambrian tectonothermal events and crustal evolution of South China: an introduction. J. Asian Earth Sci. 222, 104935.
Zhao, J.H., Zhou, M.F., 2007. Geochemistry of Neoproterozoic mafic intrusions in the Panzhihua district (Sichuan Province, SW China): implications for subduction-related metasomatism in the upper mantle. Precambr. Res. 152, 27–47.
Zhao, J.H., Zhou, M.F., 2008. Neoproterozoic adakitic plutons in the northern margin of the Yangtze Block, China: Partial melting of a thickened lower crust and implications for secular crustal evolution. Lithos 104, 231–248.
Zhao, J.H., Zhou, M.F., 2013. Neoproterozoic high-Mg basalts formed by melting of ambient mantle in South China. Precambr. Res. 233, 193–205.
Zhao, J.H., Zhou, M.F., Li, J.W., Wu, F.Y., 2008. Association of Neoproterozoic A- and I-type granites in South China: Implications for generation of A-type granites in a subduction-related environment. Chem. Geol. 257, 1–15.
Zhao, J.H., Zhou, M.F., 2009. Melting of Newly Formed Mafic Crust for the Formation of Neoproterozoic I-Type Granite in the Hannan Region, South China. J. Geol. 117, 54–70.
Zhao, J.H., Zhou, M.F., Yan, D.P., Zheng, J.P., Li, J.W., 2011. Reappraisal of the ages of Neoproterozoic strata in South China: No connection with the Grenvillian orogeny. Geology 34, 299–302.
Zhao, J.H., Li, Q.W., Liu, H., Wang, W., 2018. Neoproterozoic magmatism in the western and northern margins of the Yangtze Block (South China) controlled by slab subduction and subduction-transform-edge-propagator. Earth Sci. Rev. 187, 1–18.
Zhao, J.H., Nebel, O., Johnson, T.E., 2021. Formation and evolution of a neoproterozoic continental magmatic Arc. J. Petrol. 62, egab029.
Zheng, Y.F., Zhang, S.B., Zhao, Z.F., Wu, Y.B., Li, X.H., Li, Z.X., Wu, F.Y., 2007. Contrasting zircon Hf and O isotopes in the two episodes of Neoproterozoic granitoids in South China: implications for growth and reworking of continental crust. Lithos 96, 127–150.
Zheng, Y.F., Wu, R.X., Wu, Y.B., Zhang, S.B., Yuan, H.L., Wu, F.Y., 2008. Rift melting of juvenile arc-derived crust: geochemical evidence from Neoproterozoic volcanic and granitic rocks in the Jiangnan Orogen, South China. Precambr. Res. 163, 351–383.
Zhou, M.F., Kennedy, A.K., Sun, M., Malpas, J., Lesher, C.M., 2002b. Neoproterozoic arc-related mafic intrusions along the northern margin of South China: implications for the accretion of Rodinia. J. Geol. 110, 611–618.
Zhou, J.B., Li, X.H., Ge, W.C., Liu, Y., 2007. Geochronology, mantle source and geological implications of Neoproterozoic ultramafic rocks from Yuanbaoshan Area of Northern Guangxi. Geol. Sci. Technol. Information 26, 11–18 in Chinese with English abstract.
Zhou, J.L., Li, X.H., Tang, G.Q., Gao, B.Y., Bao, Z.A., Ling, X.X., Wu, L.G., Lu, K., Zhu, Y. S., Liao, X., 2018. Ca. 890 Ma magmatism in the northwest Yangtze block, South China: SIMS U-Pb dating, in-situ Hf-O isotopes, and tectonic implications. J. Asian Earth Sci. 151, 101–111.
Zhou, J.C., Wang, X.L., Qiu, J.S., Gao, J.F., 2004. Geochemistry of Meso- and Neoproterozoic mafic–ultramafic rocks from northern Guangxi, China: arc or plume magmatism? Geochem. J. 38, 139–152.
Zhou, J.C., Wang, X.L., Qiu, J.S., 2009. Geochronology of Neoproterozoic mafic rocks and sandstones from northeastern Guizhou, South China: coeval arc magmatism and sedimentation. Precambr. Res. 170, 27–42.
Zhou, M.F., Yan, D.P., Kennedy, A.K., Li, Y.Q., Ding, J., 2002a. SHRIMP U-Pb zircon geochronological and geochemical evidence for Neoproterozoic arc-magmatism along the western margin of the Yangtze Block, South China. Earth Planet. Sci. Lett. 196, 51–67.
Zhou, M.F., Yan, D.P., Wang, C.L., Qi, L., 2006. Subduction-related origin of the 750 Ma Xuelongbao adakitic complex (Sichuan Province, China): implications for the tectonic setting of the giant Neoproterozoic magmatic event in South China. Earth Planet. Sci. Lett. 248, 286–300.
Zhou, Y., Zhong, H., Li, C., Ripley, E.M., Zhu, W.G., Bai, Z.J., Li, C., 2017. Geochronological and geochemical constraints on sulfide mineralization in the Qingmingshan mafic intrusion in the western part of the Proterozoic Jiangnan orogenic belt along the southern margin of the Yangtze craton. Ore Geol. Rev. 90, 618–633.
Zhu, W.G., Zhong, H., Deng, H.L., Wilson, A.H., Liu, B.G., Li, C.Y., Qin, Y., 2006. SHRIMP zircon U-Pb age, geochemistry, and Nd–Sr isotopes of the Gaojiacun mafic–ultramafic intrusive complex, Southwest China. Int. Geol. Rev. 48, 650–668.
Zhu, W.G., Zhong, H., Li, X.H., Liu, B.G., Deng, H.L., Qin, Y., 2007. ^{40}Ar-^{39}Ar age, geochemistry and Sr-Nd-Pb isotopes of the Neoproterozoic Lengshuiqing Cu-Ni sulfide-bearing mafic-ultramafic complex SW China. Precambr. Res. 155, 98–124.
Zhu, W.G., Zhong, H., Li, X.H., Deng, H.L., He, D.F., Wu, K.W., Bai, Z.J., 2008. SHRIMP zircon U-Pb geochronology, elemental, and Nd isotopic geochemistry of the Neoproterozoic mafic dykes in the Yanbian area, SW China. Precambr. Res. 164, 66–85.
Zhu, W.G., Zhu, W.G., Li, Z.X., Bai, Z.J., Yang, Y.J., 2016. SIMS zircon U-Pb ages, geochemistry and Nd–Hf isotopes of ca. 1.0 Ga mafic dykes and volcanic rocks in the Huili area, SW China: Origin and tectonic significance. Precambr. Res. 273, 67–89.